UNITED NATIONS UNIVERSITY
UNU-GTP
Geothermal Training Programme
Orkustofnun, Grensasvegur 9,
IS-108 Reykjavik, Iceland

Reports 2015
Number 20

INTERPRETATION OF GEOCHEMICAL DATA FROM LOW-TEMPERATURE GEOTHERMAL AREA FLJÓTIN, N-ICELAND, COMPARED TO SELECTED GEOTHERMAL SAMPLES FROM RUNGWE TANZANIA

Nyaso Makwaya
Ministry of Energy and Minerals
754/33 Samora Avenue
P. O. Box 2000
Dar es Salaam,
TANZANIA
nyasomakwaya@yahoo.com

ABSTRACT

The chemical analysis of geothermal water requires proper sample collection, analysis, and presentation of the data. The interpretation and evaluation of all available information regarding the geochemistry are accomplished by the methods of Na-K-Mg ternary diagram, Cl-SO_4-HCO_3 ternary diagram, geothermometers, WATCH programme and Suffer 12.6.963 software. Data samples from Fljótin-Iceland are analysed pertaining to their geochemistry surface exploration and compared to selected data from Rungwe geothermal area from Tanzania. The geothermal fields differ according to volcanic activities, rock types and mineral composition. Fljótin are low-temperature geothermal field while Rungwe is classified as high-temperature geothermal field at Ngozi-Songwe (northern system) and a low-temperature field at Kiejo-Mbaka (southern system). The reservoir temperatures at Fljótin are estimated by Na-K-Mg ternary diagram in the range of 120°C -160°C and confirmed with geothermometers with temperature range; 74-136°C (chalcedony) and 64-158°C (Na/K). The mineral saturation stated were calculated by chalcedony temperature where calcite and anhydrite are saturated but not precipitating while amorphous silica is under saturated. The estimated reservoir temperature at the Rungwe volcanic zone are 130-200°C by Na-K-Mg ternary diagram, which is in agreement with quartz and K/Mg geothermometers at a temperature range of 119-154°C and 106-252°C respectively. Detailed study of the Rungwe thermal fluid chemistry is required in order to be satisfied for direct or indirect use, due to its high concentration of CO_2 which can affect the utilization of the fluid, both fields have a potential for geothermal utilization. Fljótin on the other hand can be used directly due to its low total dissolved elements and low-temperature.

1. INTRODUCTION

Global pollution has increased awareness of the detrimental environmental effects that results from burning of fossil fuel for power generation and an increasing global interest is sparked towards using

green renewable energy source such as geothermal energy. Currently, Tanzania has put more efforts towards affordable and sustainable energy by increasing the number of experts for developing the geothermal resource.

Geochemistry studies play an important role in developing geothermal field from the exploration stage, for the purpose of management and monitoring of the field. Normally geochemical exploration provides information of subsurface composition, temperature, contribution to conceptual model which contain origin of geothermal fluid and flow direction, reservoir location and boiling (Arnórsson, 2000). Furthermore, it will provide information required during production phase such as scaling deposition and corrosion which can have negative effect on operation phase as well as on the environment.

Generally, geochemistry deals with geothermal fluid composition (that is aqueous solution and gaseous steam) that reflect the thermal condition at depth which are controlled by equilibrium with minerals in the aquifer rock. Data sampling, analysis and interpretation play paramount importance in geochemistry studies of geothermal fluids.

The major types of geothermal fluid are steam, gas, geothermal waters, mixed waters and steam heated surface waters. However, the types of geothermal fluid can provide different information in the geothermal field, depending on the sampling location. Steam can be useful in calculating the temperature geothermometry and state the origin of the fluid. Gas can provide information about the characteristics of the underlying geothermal system such as reservoir temperature and the direction of subsurface water flow. The geothermal water commonly provides useful information of geothermometry, origin of fluids and production properties. Mixing models are used when the sampled fluids are a mixture of different types and can be used for designing a conceptual model of the system and steam heated surface waters. According to literature, steam heated waters have never been in the deep geothermal system but provide geothermal manifestation and physical condition of geothermal system (Arnórsson, 2000).

My study will focus on data analysis and interpretation of the low-temperature geothermal field in Iceland called the Fljótin and compare it with samples from the geothermal area in the Rungwe volcanic zone, Tanzania.

2. THE ROLE OF FLUID CHEMISTRY IN EXPLORATION

Surface exploration is at its initial stage for locating and outlining geothermal fields, and a successful study will provide enough information for site development. Its achievement depends on collaboration of a team of geoscientists dealing with geological mapping, geochemical and geophysical surveys.

The main purpose of fluid chemistry in surface exploration is to predict the reservoir temperature and give preliminary assessment on the production properties, among other things chemical equilibrium, speciation, and effect of boiling, scaling and corrosion. With fluid chemistry it is also possible to map the up-flow and flow directions, define the surface area of the reservoir, and obtain information on the origin of the fluid (Figure 1). This chapter tells about the role of the fluid chemistry in surface exploration and the tools one can use to obtain this goal.

2.1 Data sampling and quality

The collection of water samples plays an important role in developing the conceptual model for geothermal system as well as for monitoring and environmental control. Therefore, data sampling requires well trained personnel with insight into possible errors and interferences (Arnórsson, 2000). This will be further discussed in Section 5.

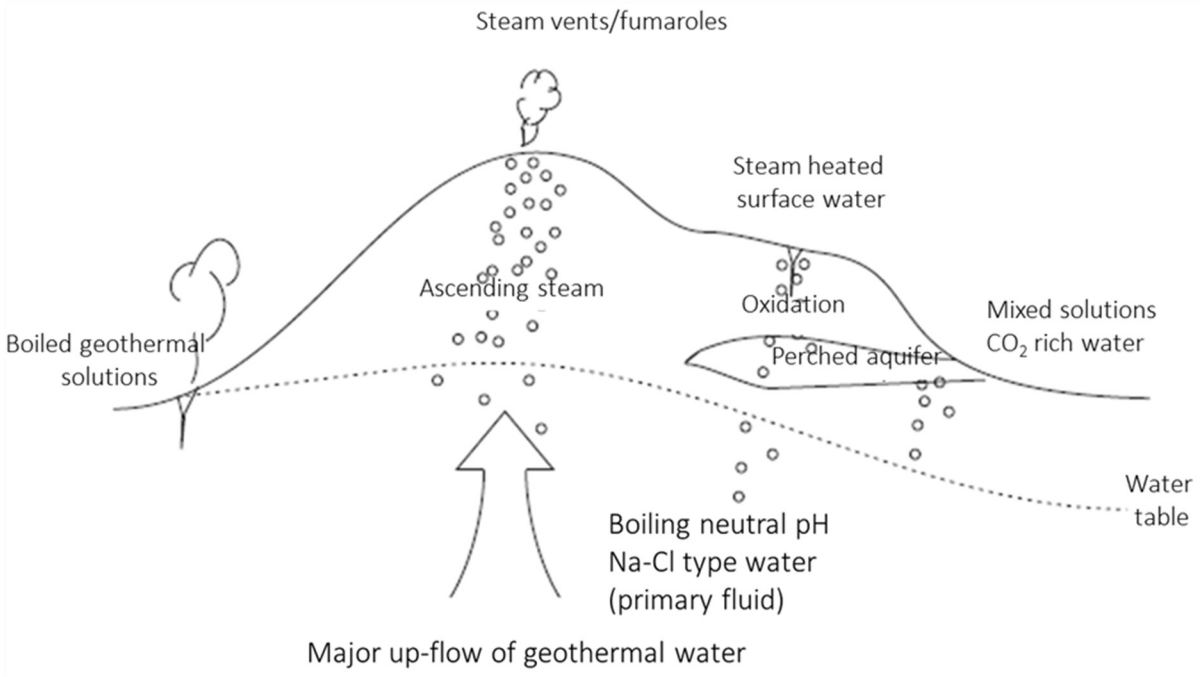

FIGURE 1: Types of geothermal fluids (modified from Arnórsson et al., 2007).

2.2 Water classification

The composition of water in geothermal field have their own characteristics depending on the rock composition, the residence time of the water within the rocks, the rate of leaching of components from the rocks, the fluid flow into the system, the rate of formation of secondary minerals, pressure and temperature. Cooling due to boiling, conduction and dilution as well as degassing, cause the chemistry of surface discharges to deviate from the composition of the thermal water in the reservoir (Arnórsson, 2000).

Ellis and Mahon (1977) has divided water into two categories: subsurface water and geothermal water respectively. Subsurface water is described as meteoric water, ocean water, carbonate water formed in young marine sediments, magmatic water and juvenile water. Geothermal water is described as water formed by reaction between the fluid and the host rock which may contain alkali-chloride water with pH 4-11, acid sulphate water and bicarbonate water.

In geothermal exploration the waters are classified regarding their composition and equilibration with geothermometry (Giggenbach, 1988). Also very useful classification is obtained by plots on ternary diagrams and other methods described below.

2.3 The Na-K-Mg ternary diagram

The nature of geothermal industry contributes many challenges on classifying fluid composition through different methods. Giggenbach (1986) developed the Na-K-Mg ternary diagram which has two areas: full-equilibrium line and "partial equilibrium, dilution or mixing" that contain Na-K-isotherms (T_{Na-K}) which may reflect deeper fluid, effective Na-K-equilibration conditions (Figure 2). The diagram is based on the temperature dependence of the three reactions shown in Equations 1, 2, and 3. Equation 4 shows the calculated sum of a large number of samples simultaneously plotted on the diagram. The area near the Mg-corner) will not apply to reflect fluid-rock equilibrium and only (T_{K-Mg}) can be used as a measure for fluid-rock equilibration temperatures by Equation 5. The Na-K-Mg ternary diagram (Giggenbach,

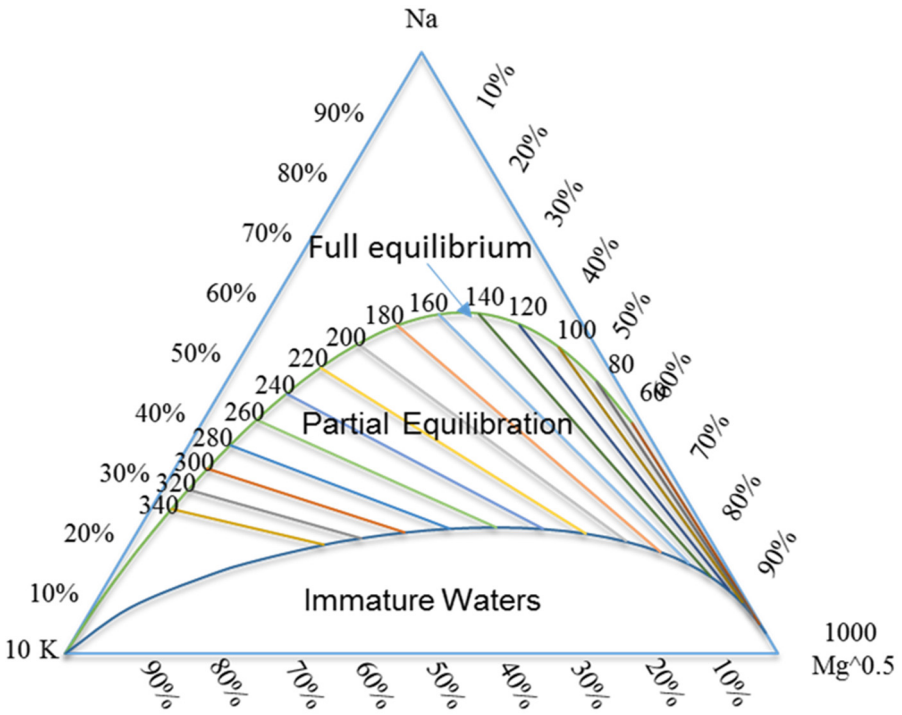

FIGURE 2: Na-K-Mg ternary diagram (Giggenbach, 1986)

1986; 1988) shown in Figure 2 can be used to classify water into equilibrium, partial equilibrium and immature waters (dissolution of rock with little or no chemical equilibrium). The full equilibrium curve is for reservoir water composition corrected for loss of steam owing to decompression boiling. Uncorrected boiled waters will generally plot slightly above the full equilibrium line. The diagram can be used to better clarify the origin of the waters and then determine whether the fluids has equilibrated with hydrothermal minerals and to predict the equilibrium temperatures by $T_{Na\text{-}K}$ and $T_{K\text{-}Mg}$:

$$K - feldspar + Na^{+} = Na - feldspar + K^{+} \quad (1)$$

$$2\,albite + 0.8K - feldspar + 1.6H2O + Mg^{2+} = 0.8mica + 0.2chlorite + 5.4silica + 2Na^{+} \quad (2)$$

$$2.8K - feldspar + 1.6H2O + Mg^{2+} = 0.8mica + 0.2chlorite - 5.4silica + 2K^{2+} \quad (3)$$

A large number of samples can be plotted simultaneously on this diagram, and mixing trends and grouping predicted. The sum is calculated as:

$$S = C_{Na/1000} + C_{K/100} + \sqrt{C_{Mg}} \quad (4)$$

Then the %Na, %K and %Mg, can be calculated as

$$\%Na = \frac{C_{Na}}{10S};\ \ \%K = \frac{C_K}{S}\ \ and\ \ \%Mg = \frac{100\sqrt{C_{Mg}}}{S}$$

where C is in mg/L.

The K-Mg geothermometer equation where calculated by Giggenbach (1991):

$$T_{K-Mg}(°C) = 4410/(14.0 - \log(K^2/Mg) - 273.15 \quad (5)$$

where *K* and *Mg* refer to the concertation's of the respective cations.

Analysis of Na, K and Mg, by using the ternary diagram will give clear distinction between waters suitable or unsuitable for the application of ionic solute geothermometers.

2.4 The Cl-SO_4 -HCO_3 ternary diagram

Giggenbach (1991) proposed a Cl-SO_4 -HCO_3 ternary diagram (Figure 3) for the initial classification of geothermal solutions to identify whether the geothermometers are applicable for the given water sample, as most solute geothermometers work only for neutral water or matured water that is characterized by high Cl and low SO_4 (Sekento, 2012). This diagram is helpful in providing an initial indication of mixing relationships or geographical groupings.

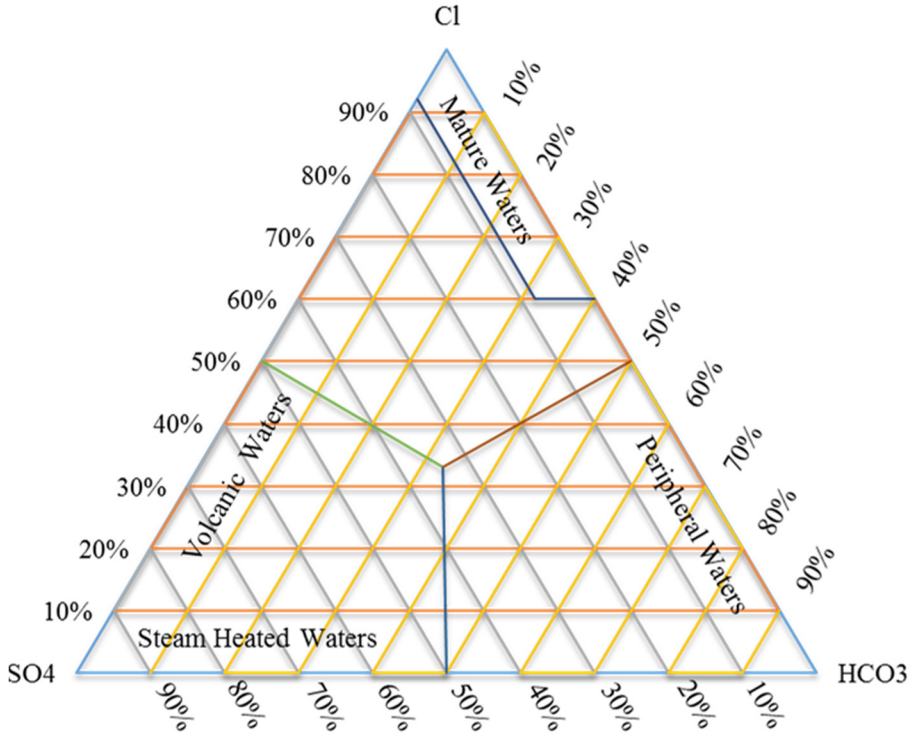

FIGURE 3: Cl-SO4-HCO3 ternary diagram

The position of a data point in such a triangular diagram is obtained by first obtaining the sum S of the concentration of all three constituents involved. In the present case:

$$S = C_{Cl} + C_{SO_4} + C_{CHO_3} \quad (6)$$

The next step consists of the evaluation of %Cl, %SO_4 and %HCO_3 according to the following:

$$\%Cl = 100C_{Cl;}\ \ \%SO_4 = 100C_{SO_4/S;}\ \ \%HCO_3\ = 100C_{HCO_3/S}$$

The degree of separation between data points for high chloride and bicarbonate water gives an idea of the relative degree of interaction of CO_2 charged fluids at lower temperatures and the HCO_3 contents increasing with time and distance travelled. The geothermometer can only be used with close neutral water which contain Cl as major anion.

2.5 Geothermometers

According to Arnórsson (2000), geothermometers have been classified in three groups; water or solute

geothermometer, steam or gas geothermometer and isotope geothermometer where water and steam are termed collectively as a chemical geothermometer. In addition to that, Sekento (2012) reported that equilibrium between minerals, geothermal solutions and vapour phase can affect the chemical composition of geothermal fluids, providing the basis for chemical geothermometer. Chemical geothermometer are normally applied to thermal springs, steam vents and geothermal wells. The effect of boiling and cooling geothermometry is used to elucidate the chemical reaction occurring in the zone of depressurization around wells that result from recharging cold water (Arnórsson, 2000). The most widely used geothermometer are based on silica concentration (quartz and chalcedony), cation ratios (Na/K, K/Mg and Na-K-Ca) based on equilibration on Na-K-Mg. Below I describe and discuss the geothermometers used in this paper/work.

2.6 Silica geothermometers

The silica solubility increases with temperature rise, which tend to control the silica in the geothermal fluid. The common geothermometer temperature predicted by silica are referred as quartz, amorphous silica and chalcedony temperatures. The amorphous silica method is recommended for 25-250°C range, chalcedony for water in the subsurface temperature range of 120°C-250°C, while quartz is recommended above 200°C (Arnórsson, 2000). The basic reaction for the dissolution of silica minerals is:

$$SiO_{2(s)} + 2H_2O = H_4SiO_{4(aq)} \quad (7)$$

At pH levels below 9, nearly all dissolved silica is present in solution as dissociated silicic acid, H_4SiO_2. At higher pH levels, the silicic acid dissociates to form H_3SiO_4, thus effectively increasing the solubility of silica in water in equilibrium with quartz. Therefore, very high pH levels can lead to over-estimation of the reservoir temperature if the aqueous speciation of silica is not considered. However, several geothermometers have been developed as more experimental data has become available (Gunnarsson and Arnórsson, 2000). Verma and Santoyo (1997) have recently developed a new silica geothermometer based on statistical treatment of earlier experimental data. Their new geothermometer is proposed through detecting an outlier and rejecting one sample from the data set of Fournier and Potter, 1982. The quartz geothermometer was tested experimentally over the temperature range from 100°C to 500°C and pressure of 1000 bars, performed well up to 400°C without any effect of fluid composition (Pope et al., 1987). However, Verma (2000) criticized the use of the quartz geothermometer, especially its discrepancy at high temperatures arising from the incoherence between the theoretical and experimental solubility data. The silica geothermometers equations used to calculate the temperature of a reservoir are as follows:

Quartz, 25-900°C (Fournier and Potter, 1982):

$$T(^oC) = -42.2 + 0.28831S - 3.6686x10^{-4}S^2 + 3.1665x10^{-7}S^3 + 77.034logS \quad (8)$$

Chalcedony, 0-250°C (Fournier, 1977):

$$T(^oC) = \frac{1032}{4.69 - logS} - 273.15 \quad (9)$$

Chalcedony (Arnórsson et al., 1983):

$$T(^oC) = \frac{1112}{4.91 - logS} - 273.15 \quad (10)$$

Amorphous silica (Fournier, 1977) for 25-250°C:

$$T(^oC) = \frac{731}{4.52 - logS} - 273.15 \quad (11)$$

where S refers to the concentration of SiO_2 in mg/kg and T is the Temperature.

2.7 Cation geothermometer

Cation geothermometer is commonly used to estimate reservoir temperatures. For the cation geothermometers, the Na-K geothermometer is most widely used, rather than K/Mg and Li-Mg (Kharaka and Mariner, 1989). The geothermometers equations used to calculate the temperature of a reservoir are as follows:

Arnórsson et al. (1983) for 25-250°C:

$$T(^{O}C) = \frac{933}{0.993 + log\frac{Na}{K}} - 273.15 \quad (12)$$

Giggenbach et al. (1988):

$$T(^{O}C) = \frac{1390}{1.75 + log\frac{Na}{K}} - 273.15 \quad (13)$$

Giggenbach et al. (1988):

$$T(^{O}C) = \frac{4410}{14.0\ - \mathrm{og}(\frac{K^2}{Mg})} - 273.15 \quad (14)$$

2.8 Mineral saturation

Mineral saturation is applied in geochemistry to obtain an understanding of various physical features of a geothermal system through specific minerals which are in chemical equilibrium. The saturation index of several minerals is computed as a function of temperature and if the saturation indices of the minerals converge to zero (saturation) at a specific temperature that the temperature is taken to present the reservoir temperature. Using the result of the aqueous speciation calculations, the saturation indices (SI) of minerals in aqueous solutions at different temperatures were computed as in Equation 15:

$$SI = loqQ - logK = log\ Q/K \quad (15)$$

where Q is the calculated ion activity product and K is the equilibrium constant.

The SI value for each mineral is a measure of the saturation state of the water phase with respect to the mineral's phase. Values of SI greater than, equal to, and less than zero represent super saturation, equilibrium and under saturation respectively, for mineral phase with respect to aqueous solution. Equilibrium constants for mineral's dissolution often varies strongly with temperature, that temperature taken to be the reservoir temperature. The WATCH computer program version 2.1A (Arnórsson et al., 1982) is commonly used for calculation of mineral saturation index.

3. ICELAND – GEOLOGICAL BACKGROUND

3.1 Regional geology

Iceland is young volcanic island with the oldest rocks about 16 million year old according to radiometric dating. The volcanic activity in Iceland is high with the eruption frequency of over 20 events per century with a magma output of over 5 km^3 (Hjartarson and Saemundsson, 2014). The lava flows cover more than 2000 km^2. The volcanic activities have been contributed to the complex interaction between the N-Atlantic Ridge system and the Iceland Mantle Plume in the mid oceanic ridge which has generated a complex tectonic situation (Hjartarson and Saemundsson, 2014). The location of Iceland at the

asthenospheric flow under the NE-Atlantic plate boundary interacts and mixes with a deep-seated mantle plume that contributes to volcano activities (Schlitzer et al., 1985) with series division of postglacial (last 9000 to 13000 years), upper Pleistocene (back to 0.7 million years), Plio–Pleistocene (0.7-3.1 million years) and Tertiary rocks older than 3.1 million years (Hjartarson and Saemundsson, 2014).

The buoyancy of the Icelandic plume leads to a dynamic uplift of the Iceland plateau and high volcanoes over the plume produce a relatively thick crust. The Greenland – Faeroe ridge represents the Icelandic plume track through the history of the NE-Atlantic. The two main volcanic belts are connected in central Iceland by the Hofsjökull volcanic system (Hjartarson and Saemundsson, 2014) (Figure 4). The northern end of the eastern main volcanic belt is connected to the crested zone of the Mid Atlantic Ridge by active transverse faults. In southern Iceland this volcanic belt is propagating south; at the same time dilation is dying out in the northern half of the western main volcanic belts. The main volcanic belts in Iceland are displaced relative to the crest zone of the mid Atlantic Ridge because the lithosphere tends to break up above the mantle plume and the plume has been moving east relative to the plate boundary (Saemundsson, 1979).

North and northwest Iceland are composed of tertiary basalt formation, except for the outlying and extinct Skagi volcanic belt which was formed during the Plio – Pleistocene time. The age of the Tertiary basalt formation ranges from about 12 million years in the deepest part of the stratigraphically column at the northern tip of Tröllaskagi to about 7 million years in the region from Blönduós across the central highlands to the bottom of Eyjafjardardalur (Hjartarson and Saemundsson, 2014). The volcanic activities are the major factor in identifying the geothermal system.

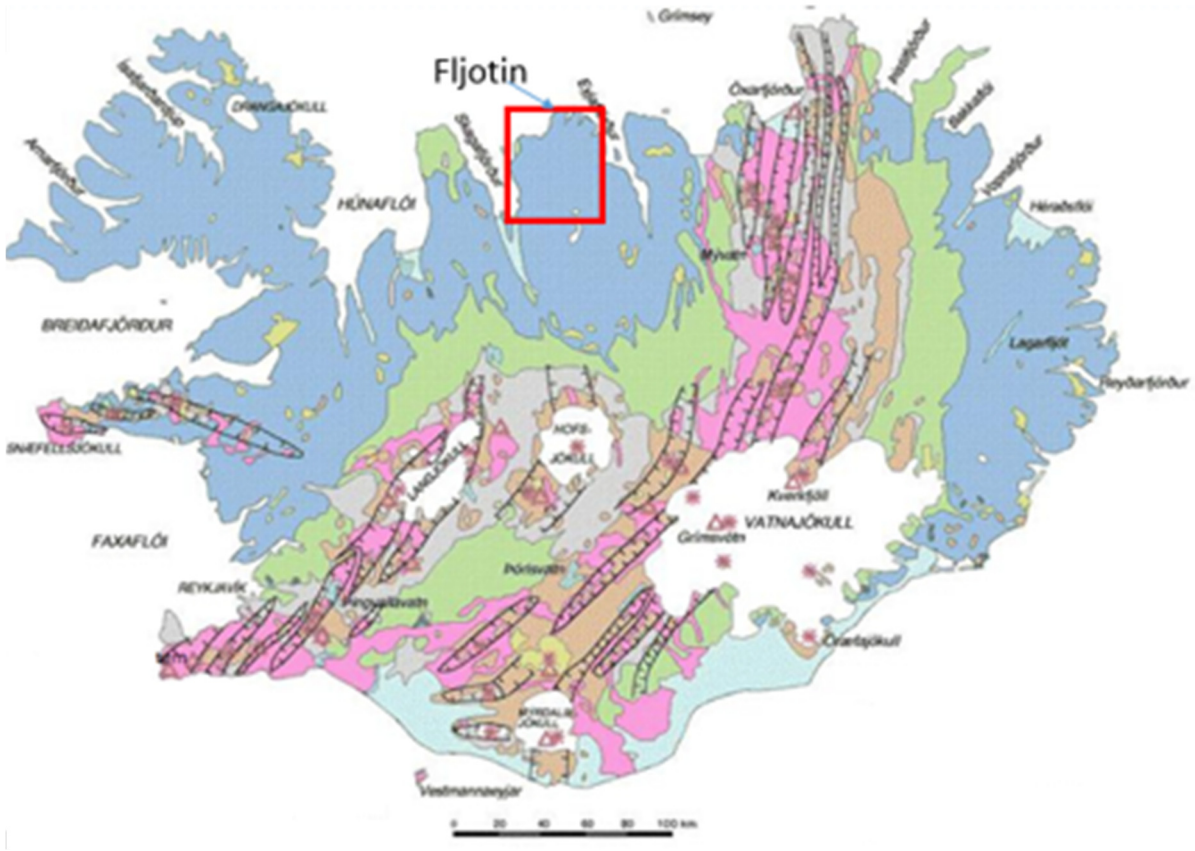

FIGURE 4: A simplified geological map of Iceland showing the volcanic zones, fissures swarms and central volcanoes (Jóhannesson and Saemundsson, 1999). The box represents the study area of Fljótin

3.2 Geothermal systems in Iceland

Several classification schemes have been proposed for geothermal systems. The most used terms are; high-temperature and low-temperature geothermal systems, hot water (liquid dominated) and vapour dominated system and volcanic and non-volcanic systems as described below. High temperature systems are generally volcanic and low-temperature systems non-volcanic.

The first classification is based on the physical state of reservoir fluid, where the geothermal system is classified as liquid-dominated reservoirs when the temperature is at or below boiling point, while water phase controls pressure (hydro-static). Two-phase reservoirs where the fluid temperature and pressure follow the boiling point curve. The second one is based on vapour-dominated reservoirs where the temperature will be at or above boiling point, while steam phase controls pressure (vapour-static) (Nicholson, 1993).

The third classification is based on geological conditions of the system. They can be volcanic systems, which are associated with volcanic activity (hot intrusions/magma), secondly it can be convective fracture controlled systems where hot crust occurs at depth in tectonically active areas, thirdly it can be sedimentary systems where permeable layers occur at great depth or have above average heat flow. Fourthly, geo-pressured systems with stratigraphic sedimentary "traps" and lastly enhanced (EGS) systems where reservoir permeability is enhanced or created, previously "hot dry rock" (HDR) systems. In addition to that, there are shallow resources that are utilized through ground-source heat-pumps (Nicholson, 1993).

Based on geological settings and temperature from geothermal fields, the geothermal areas in Iceland are classified as high- or low-temperature geothermal fields. The high–temperature are located within volcanic belts in the central part of the country whereas most of the low -temperature occur in the quaternary and tertiary formation (Arnórsson, 1995).

3.2.1 Fljótin, N-Iceland

Fljótin (Figure 5) is a district located in north Iceland on the northern part of Tröllaskagi, a mountainous peninsula between two ocean fjords called Skagafjördur to the west and Eyjafjördur to the east. The whole part of Fljótin is covered by basaltic lavas and minor intermediate extrusive rocks and sedimentay horizons (Hjartarson and Saemundsson, 2014). The bedrock in the Fljótin district is tertiary in age, tholeiitic basalts in composition. The lava pile has a westerly dip and the mountainous strata is near totally composed of lavas with only minor sedimentary horizons. Dykes

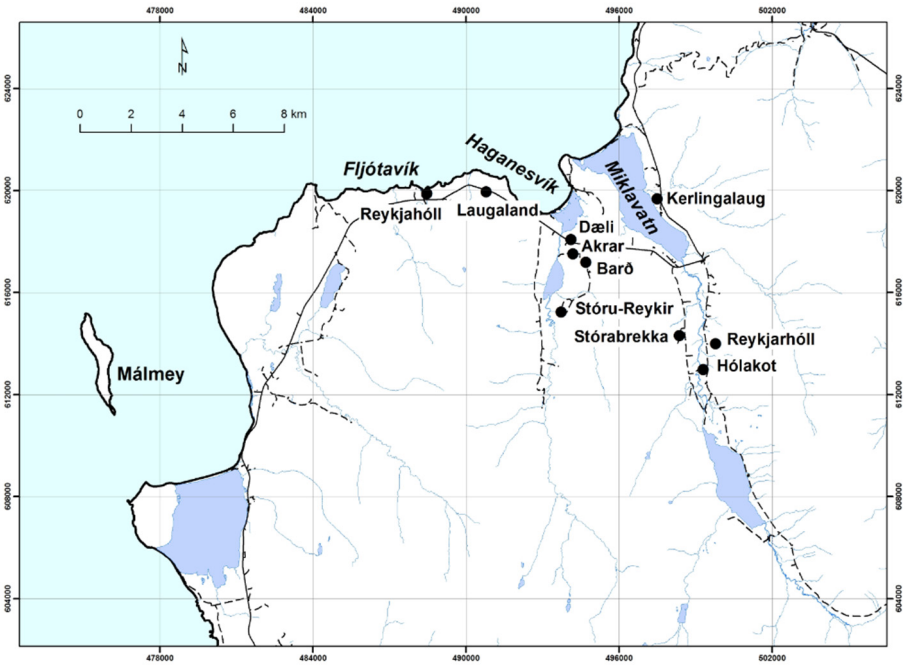

FIGURE 5: Location of the thermal springs in Fljótin used in this project (Map drawn by Jónsdóttir, 2015)

generally trend near N10°E and are rare in Fljótin district but more numerous to the northeast. Large N-S faults are observed north of Miklavatn, and such faults are likely to be present in the western part of Fljótin. The pores in the lavas are mostly filled by deposition reducing the permeability and it is likely that permeability of geothermal systems are largely related to fractures, faults and dykes. The area is low-temperature liquid dominated with widespread distribution of warm springs (25-50°C) and hot springs (50-75°C) of which few are shown in Figure 5 and in Table 1. Fljótin are flat lowlands and covered by green vegetation (Jóhannesson, 1991).

The young rock is the main heat source for the Fljótin low-temperature field. Rainwater from the surrounding high mountainous area, reaching above 1000 m above sea level, seeps through the north-south trending faults down to hot rocks at a temperature around 150°C. Normally rainwater has lower density than cold water, then after being heated by the hot rock it flows up to reach the surface at temperature around 60-70°C (Sæmundsson, pers. comm. 2015). Thermal springs are widespread in the area which is shown in Figure 5 and fluid composition in Table 1.

TABLE 1: Fluid composition from Fljótin (samples collected in October 1985)

Name	Sample No	Temp. surface (°C)	pH/°C	CO_2	H_2S	SiO_2	Na	K	Mg	Ca	Cl	SO_4	F	dO_{18}	Conductivity/ 25°C	Charge balance
Bardslaug (1)	19850276	66.5	9.76/22.0	18.9	0.49	135.7	77.3	1.96	<0.001	1.77	29.23	53.63	0.62	-12.22	385	-0.24
Bardslaug (1*)	19730114	-	9.78/20.0	24.2	<0.10	146.0	75.3	1.9	0.060	1.63	24.80	52.7	0.70	-	-	-4.31
Daelir_(2)	19850277	46.4	9.72/22.0	20.6	0.16	142.2	80.5	2.69	0.005	2.3	29.65	56.5	0.61	-12.43	402	2.49
Akrar_(3)	19850278	61.0	9.7/22.2	20	0.23	147.1	78.7	2.71	0.004	1.77	29.68	56.32	0.63	-12.31	395	-0.08
Reykir (4)	19850279	48.8	10.2/22.5	13.4	0.10	90.4	65.2	0.87	0.001	2.09	22.50	40.15	0.53	-12.31	338	-5.31
Laugaland_(5)	19850280	64.7	9.85/22.3	18.9	<0.10	95.9	61.0	1.08	0.015	0.28	21.48	34.83	0.62	-12.33	304	-0.97
Reykjarhóll á Bökkum - well (6)	19850281	57.5	9.64/22.4	23.6	0.95	147.8	76.2	2.42	<0.001	2.41	29.89	50.79	0.73	-12.11	381	-0.43
Kerlingalaug_(7)	19850282	55.5	9.98/23.0	18.8	0.53	94.2	62.6	0.98	<0.001	1.86	22.45	35.3	0.59	-11.97	321	-3.98
Kerlingalaug (7*)	19690130	49.0	9.45/22.0	18.5	0.58	97.0	76.5	2.37	0.040	1.78	24.20	34.7	0.60	-	-	51.48
Hólakot_(8)	19850283	23.8	10.16/22.5	14.6	0.15	101.5	50.1	0.86	0.063	2.05	8.55	19.69	0.50	-12.21	252	-3.96
Reykjarhóll east (9)	19850284	52.8	10.19/22.7	14.1	0.17	102.8	51.3	0.8	<0.001	1.78	8.78	19.76	0.51	-12.19	255	-5.61
Reykjarhóll east (9*)	19690128	58.0	9.74/22.0	13.5	0.16	107.0	50.0	0.87	0.030	1.66	9.10	20.1	0.60	-	-	50.86
Stóra-Brekka (10)	19850285	88.5	10.21/22.5	8.2	0.13	52.0	74.7	0.32	<0.001	4.53	36.28	72.01	0.42	-12.67	406	-2.62
Stóra-Brekka (10*)	19690131	55.0	9.71/22.0	13	<0.10	87.0	65.5	1.1	0.08	1.94	23.4	38.5	0.40	-	-	36.92

Samples (1, 7, 9, and 10) have Mg value below detection limits therefore author uses 0.001 mg/L in these samples in diagrams
Number in brackets represent the numbers in ternary diagrams. All sample are hot springs except for sample number 6 which is from a well
- Not analysed

4. TANZANIA GEOLOGICAL BACKGROUND

Tanzania is part of East African countries along the Indian Ocean. "The youngest sediments and volcanic are related to the active Cenozoic East African Rift System (EARS). The location of the Cenozoic EARS is strongly controlled by Proterozoic tectonics and Karoo rift geometry with both Eastern and Western branch following the margins of the Archean Tanzania craton" (Ebinger et al., 1989), e.g. Figure 6. The two branches form a junction in southern Tanzania which has been the location of intensive eruption in Holocene time, producing basalt, phonolite and phonolitic trachyte lavas which have erupted from numerous centres and had significant trachytic

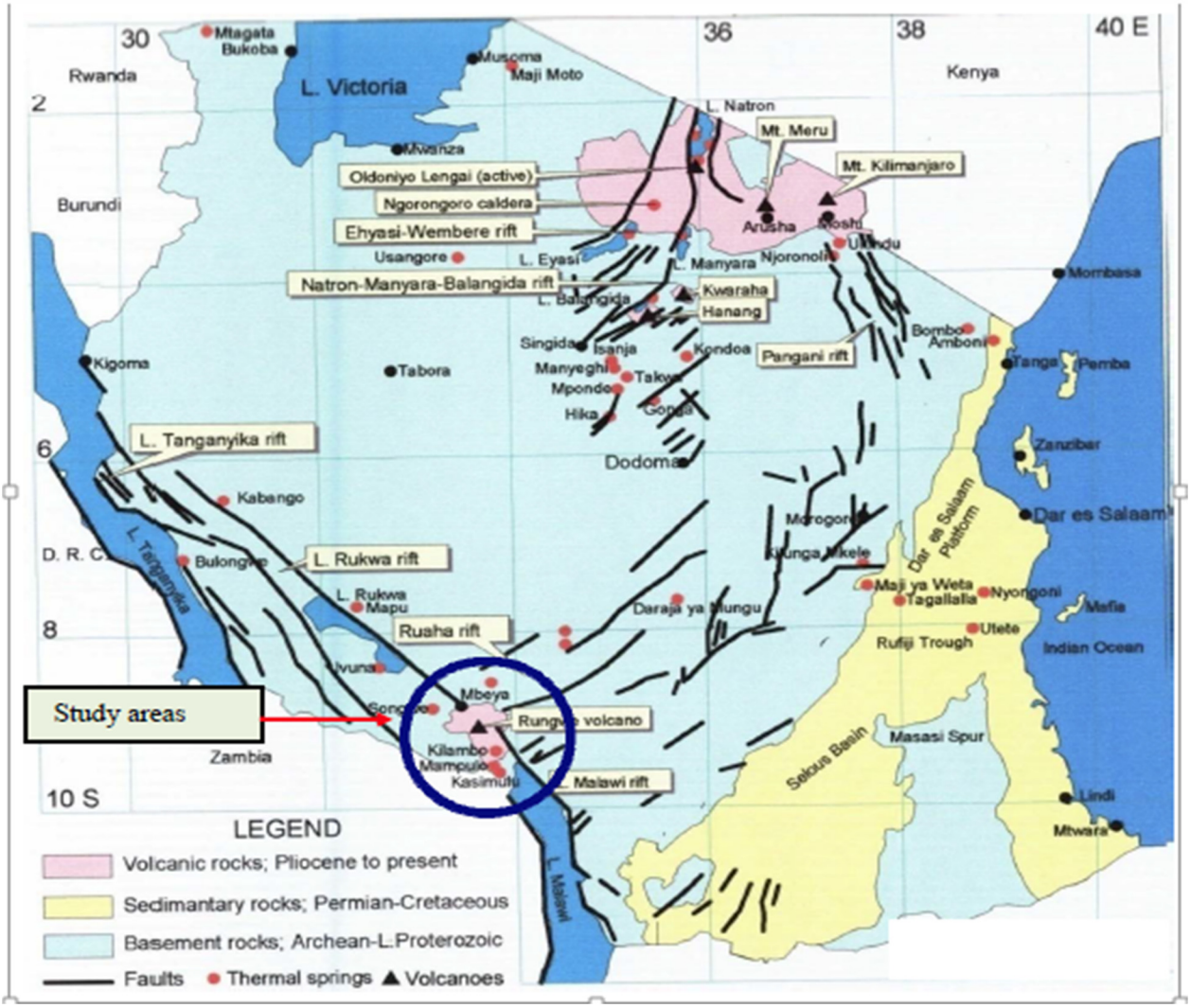

FIGURE 6: Geothermal site, study area and the rifting system in Tanzania. The blue ring represents Rungwe volcanic zone with selected thermal springs used in this report (Mwihava, 2004)

explosive eruptions. Two eruptions were dated ca.10-12 ka (plinian-style eruption: Kitulo Pumice) and < 1ka (Ignimbrite-forming eruption: Ngozi Tuff (Ochmann and Garofalo, 2013).

The geology of Tanzania is dominated by the Archean Craton, a stable continental nucleus, which covers most of central and western Tanzania. Tanzania craton is the Paleoproterozoic Ubendian Belt and the southeast the Paleoproterozoic Usagara Belt, which are dominated by a variety of high to medium grade metamorphic rocks of both sedimentary and igneous origin. Holocene volcanism has taken place in three main large volcanoes of the RVP, Ngozi, Rungwe and Kiejo (Ochmann and Garofalo, 2013).

4.1 Rungwe volcanic zone

The area of investigation belongs to the Rungwe Volcanic Province in Mbeya as shown in Figure 6 and Figure 7. The Mbeya area is located at the intersection between the western and eastern branches of the East African Rift system (EARS) forming a triple junction. The area is characterised by hydrothermal surface manifestations, potential volcanic heat sources, and fault-controlled permeability favouring fluid pathways along faults associated to the East African Rift system. Additionally, there is sufficient recharge in the high elevated area for filling up the naturally lost fluid (Ochmann and Garofalo, 2013). The previous study reveal that almost 10 MW of thermal fluid is lost from Songwe hot springs

(geothermal outflow zone), which is indicating a substantial reservoir in the subsurface. Table 2 represent fluid composition of geothermal water from Rungwe.

TABLE 2: Fluid composition of Rungwe (Collected 2006-2008; Ochmann. and Garofalo, 2013)

Name	Sample number	pH	Temp °C	CO_2	SiO_2	Na	K	Mg	Ca	Cl	SO_4	Al	Fe	Li	Charge balance
Udindilwa (a)	23	7.00	82.40	854.75	72.7	893.0	28.50	3.90	13.40	82.40	247.	0.017	0.100	0.30	0.019
Ibayi (b)	29	6.80	80.20	1269.50	82.3	646.0	40.30	2.30	12.00	116.00	297.00	0.008	0.100	0.30	0.001
Main spring ER (d)	19	6.70	65.70	1441.20	71.8	775.0	95.40	15.60	30.30	197.00	154.00	0.023	0.100	0.70	0.005
Aqua Afia 3 (e)	15	6.90	60.30	1384.20	133.0	106.0	48.70	4.50	12.10	9.00	1.70	0.007	<0.100	20.60	-0.015
Aqua Afia 1 (f)	16	6.70	56.60	1990.80	124.0	100.0	46.90	5.80	15.50	8.20	1.00	0.003	<0.100	17.50	0.009
Ikumbi 2 (g)	26	6.80	54.70	2019.70	125.0	102.0	48.70	4.90	13.50	8.70	1.40	0.004	<0.100	20.60	-0.007
Kandete (h)	9	7.40	56.60	295.02	126.0	1246.0	66.00	13.90	15.50	224.00	252.00	<0.005	0.300	0.40	0.164
Kasimulo (i)	10	7.70	42.40	293.57	105.0	1218.0	68.10	15.80	26.10	204.00	317.00	<0.005	0.200	0.40	0.144
Ilatile 4 (k)	5	8.50	80.20	139.21	70.3	818.0	82.00	8.00	17.10	184.00	143.00	<0.005	0.200	0.80	0.013
Swaya (m)	12	7.20	44.10	295.02	89.5	52.1	80.40	4.80	13.10	12.50	14.00	0.019	0.027	0.00	0.162

Letters in brackets represent the numbers in ternary diagram

The triple junction of the NW-SE trending south Rukwa and North Malawi rift basin intersected by younger NE-SW trending Usangu basin is covered by Rungwe volcanic rocks. There are also a number of Cretaceous carbonatite intrusions in the Mbeya region, including the Panda Hill Carbonatite which is located between Ngozi Volcano and Songwe hot springs. The condition for high enthalpy resources are principally favourable in the Mbeya region due to the presence of active faults which allow fluid flow, young volcanic heat sources (which are sparse in other areas of western branch of the east African system) and the occurrence of surface manifestations, such as hot springs, indicating geothermal subsurface activity (Ochmann and Garofalo, 2013). Figure 7 indicate the hot spring sample selected for Rungwe area.

The Rungwe volcanic zone has been divided into two geothermal fields; Northern geothermal system (Ngozi-Songwe) which is high temperature field (>200°C) and Southern geothermal system which is low-temperature field (<200°C) (Ochmann and Garofalo, 2013).

FIGURE 7: Locations of selected samples form Rungwe area used in this work. The map is from the geothermal site, study area and the rifting system in Tanzania (Source: Google Earth)

5. RESULTS AND DISCUSSION

5.1 The Fljótin geothermal area

5.1.1 The charge balance evaluation

The samples from the Fljótin in north Iceland which are discussed in this report were collected in 1963, 1969, 1973 and 1985 by geoscientists from ISOR (ISOR database). At that time only the major elements were analysed and very limited interpretation been published on these data and all the reports are in Icelandic. The author of the current report calculated speciation, sample quality, and mineral saturation index (Tables 3 and 4) by using the WATCH program (Arnórsson et al., 1982).

The surface temperature indicates low-temperature geothermal field with temperature range of 23.5-88.5°C. The Fljótin data consist of 13 samples from hot springs and one from a borehole (number 6). The ID number for each sample is shown in parenthesis following the name. These are: Bardslaug (1, 1*), Daelir (2), Akrar (3), Reykir (4) Laugaland (5) Reykjarhóll á Bökkum (6) a borehole, Kerlingalaug (7, 7*), Hólakot (8), Reykjarhóll east (9, 9*), and Stóra-brekka (10, 10*). The fluid composition is shown in Table 1. The borehole is only 257.3 m deep and was drilled in February 1985 (ISOR database).

The sample quality is one of the major factors in geochemical data analysis, which could depend on factors such as sampling procedure, storage, sampling point, treatment and transportation and even climate condition. The sample quality can be evaluated by charge balance error (CBE Equation 16), is calculated from the total number of anions and cations in the fluid sample. The CBE value should be less than 5% to be regarded as an acceptable geochemical analysis – the closer to zero the better.

$$CBE(\%) = \frac{\sum Z_{cat} m_{cat} - \sum Z_{an} m_{an}}{\sum Z_{cat} m_{cat} + \sum Z_{an} m_{an}} x100\% \quad (16)$$

Where Z_{cat} and Z_{an} are charge of the cation and the anion, m_{cat} and m_{an} represent concentration of an element.

The charge balance error states the sample quality during collection and total composition of charges anions and cations (Table 1). Five of the samples from Fljótin of seven samples have CBE value in the range > 5 –51. The CBE for Kerlingalaug (7*) is 51.48%, Reykjahóll East (9*) is 50.86% and Stóra-Brekka (10*) is 36.92% which are too high for sample quality analysis. The results for high CBE can be caused by sampling procedure, laboratory error, sample contamination, unfiltered samples, and some samples can precipitate in the container (Basu, 2008). Though the sample quality is beyond the limit value for analysis and interpretation of thermal fluid, it will be used for learning purpose with their inclusive in data analysis and interpretation. Apart from being with high CBE the samples are used due to their minor difference in concentration of major element in the samples such as H_2S, SiO_2, Na, and Cl which differ at a range of 1-5mg/L.

The Mg value for Bardslaug (1), Kerlingalaug (7), Reykjarholl East (9) and Stora Brekka (10) were almost zero value (<0.001 mg/L) or less than the detection limits which meant the sample could not be used for the Na-K-Mg ternary diagram (Giggenbach, 1986). Therefore, Mg concentration for those samples were interpolated as 0.001 mg/L. The low concentration of Mg can be caused by time difference and mixing of sample and/or different analytical methods.

5.1.2 The Na-K-Mg and the Cl-SO_4-HCO_3 ternary diagrams

The samples were plotted on Na-K-Mg ternary diagram shown in Figure 8. The reservoir temperature estimated at a temperature range of 120-160°C. The temperature range is within the range calculated by the geothermometers as shown later. Samples from Reykir (4) and Reykjarhóll á Bökkum (6) the bore hole which are both equilibrated, while Bardslaug (1*), Daelir (2), Akrar (3), Laugaland (5),

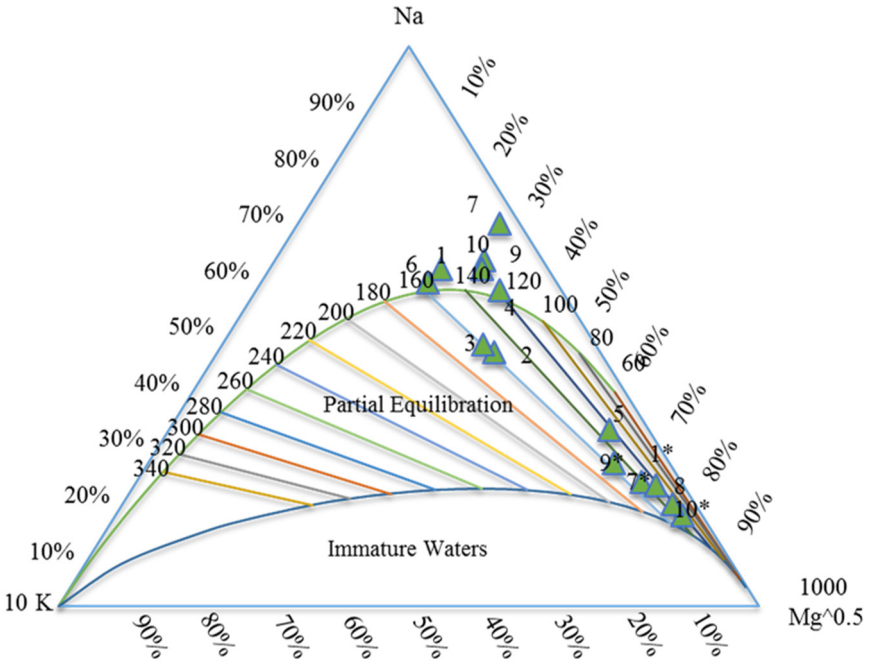

FIGURE 8. Classification of water by Na-K-Mg ternary diagram for the Fljótin samples, numbers are the same as in Table 1

Kerlingalaug (7*), Hólakot, Reykjahóll east (9*) and Stóra-Brekka (10*) are partially equilibrated. On the other hand, Bardslaug (1), Kerlingalaug (7) Reykjahóll east (9), and Stóra-Brekka (10) were beyond the equilibrated line indicated by Giggenbach (1986).

The different results from same sample like no 7 and 7* are likely affected by time difference in sample collection, and technology. The effect can be seen in Na-K-Mg ternary diagram where sample plotted above the equilibrium line and to the corner of Mg (no 7 and 7*). Also seen in Table 1.

The results from same area can give different values as can be seen on the Na-K-Mg ternary diagram (Figure 8) for chalcedony geothermometer Bardslaug (1), and (1*) has an approximate temperature of 130°C and 135°C respectively, Kerlingalaug (7) and (7*) has 107°C and 109°C respectively, Reykjarhóll East (9) and (9*) has an approximate temperature value of 112°C and 115°C respectively, and Stóra-Brekka (10) and (10*) has a temperature 74°C and 102°C respectively. The temperature difference is almost +5 or-5 which is small compared to Stóra-Brekka where difference is ~25°C. Therefore, the duplicated sample for Bardslaug, Kerlingalaug and Reykjarhóll East sampling point are considered to be agreement, where on the other hand Stóra-Brekka does not agree.

On the Cl-SO_4-HCO_3 ternary diagram shown in Figure 9 the Fljótin samples plots in the volcanic waters and close to the center of the diagram. The low concentration of Cl may indicate mixing process with rainwater and/or low Cl concentrations of the Icelandic tholeiitic basalts.

5.1.3 The geothermometers

The geothermometers are selected according to volcanic activities, rock type, and mineral composition and sampling surface temperature. The geothermometer used to calculate the reservoir temperature for Fljótin are: the quartz geothermometer by Fournier and Potter (1982), the chalcedony geothermometer by Arnórsson et al., (1983), the amorphous silica geothermometer by Fournier (1977) and the Na/K geothermometer by Giggenbach (1988). The results of the calculations are shown in Table 3.

The chalcedony geothermometer gives temperature range between 74 and 136°C, the quartz geothermometer temperature range between 104-160°C, the amorphous silica range in 10-38°C and

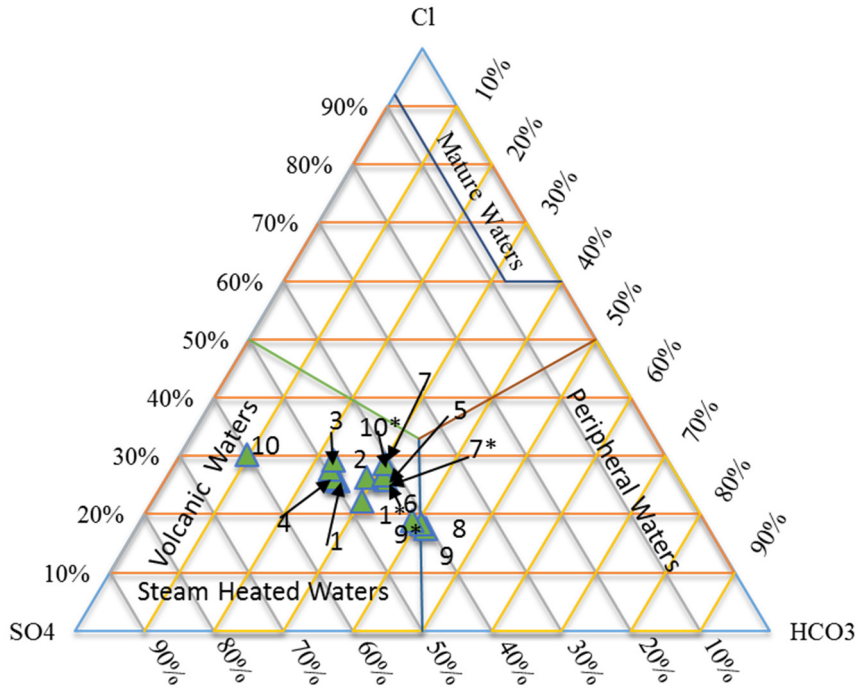

FIGURE 9: Classification of water by Cl-SO_4-HCO_3 ternary diagram for the Fljótin samples; numbers are the same as in Table 1

Na/K geothermometer temperature range was 64-158°C. The amorphous silica geothermometer gives unexpected lower temperature compared to surface temperature for such situation, as amorphous silica will not fulfil the estimation of the reservoir temperature.

The Na/K geothermometer and Na-K-Mg ternary diagram gives similar temperature value for reservoir temperature estimation. Arnórsson (1975) concluded that the Icelandic water are equilibrated with chalcedony at a temperature < 180°C. Therefore, chalcedony geothermometer is considered here to give the most likely reservoir temperature range of 74-136°C.

TABLE 3: Solute geothermometers for Fljótin samples (°C)

Sample name	Surface temperature (°C)	Chalcedony (°C) (1)	Quartz (°C) (2)	Amorphous silica (°C) (3)	Na/K (°C) (4)
Bardslaug (1)	66.5	130	155	33	142
Bardslaug (1*)	-	135	160	37	122
Daelir (2)	64.7	134	158	36	158
Akrar (3)	57.5	136	160	38	159
Reykir (4)	55.5	104	132	12	110
Laugaland (5)	52.8	108	135	15	124
Reykjarhóll á Bökkum, well (6)	88.5	136	161	38	155
Kerlingalaug (7)	48.8	107	134	14	118
Kerlingalaug (7*)	49.0	109	136	15	134
Hólakot (8)	46.4	111	138	18	122
Reykjarhóll east (9)	61.0	112	139	18	118
Reykjarhóll east (9*)	58.0	115	141	20	102
Stóra-Brekka (10)	23.8	74	104	33	64
Stóra-Brekka (10*)	55.0	102	130	10	100

Number in brackets represent the numbers in ternary diagrams

1. Arnórsson et al., 1983; 2. Fournier and Potter, 1982; 3. Fournier, 1977; 4. Giggenbach, 1988

5.1.4 The mineral saturation

According to the theory of mineral saturation, equilibrium is reached when saturation index (SI) is equal to zero, under-saturated when SI is less than zero and supersaturated when the SI is greater than zero. In Fljótin the system is under saturation with higher temperature of chalcedony by considering samples from Bardslaug (1, 1*), Kerlingalaug (7, 7*), Reykjarhóll east (9, 9*), and Stóra-Brekka (10, 10*) as in Table 4. The mineral saturation state of the Fljótin geothermal field are calculated by the chalcedony reservoir temperature by Fournier (1977) which indicate saturation for calcite and amorphous silica while under-saturation for anhydrite as shown in Figure 10. This indicates low mineral precipitation when utilizing the fluid.

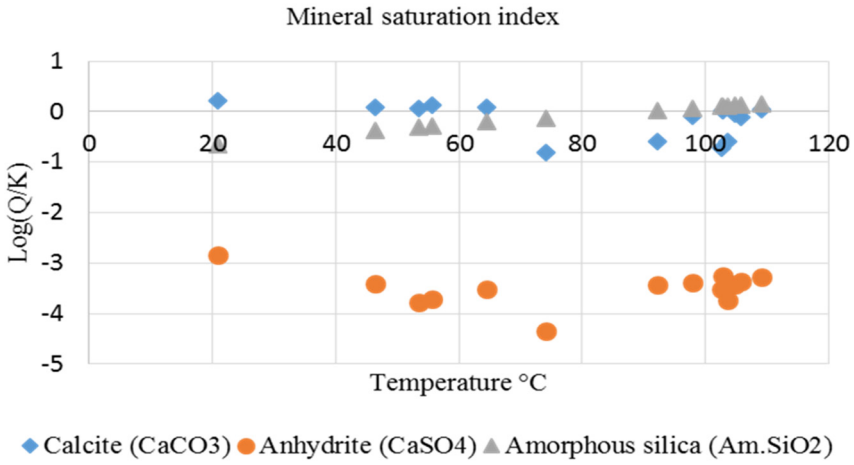

FIGURE 10: Mineral saturation state for Fljótin

TABLE 4: Mineral saturation state for Fljótin. SI index calculated at chalcedony temperature

Hot spring	Surface temperature (°C)	Chalcedony temperature (°C)	Calcite ($CaCO_3$) SI index	Anhydrite ($CaSO_4$) SI index	Amorphous silica ($Am.SiO_2$) SI index
Bardslaug (1)	66.5	97.9	-0.1	-3.38	0.065
Bardslaug (1*)	.	104.8	-0.049	-3.425	0.116
Daelir (2)	64.7	102.8	0.02	-3.25	0.101
Akrar (3)	57.5	105.7	-0.11	-3.36	0.122
Reykir (4)	55.5	46.5	0.09	-3.42	-0.383
Laugaland (5)	52.8	74.2	-0.82	-4.34	-0.125
Reykjarhóll á Bökkum well (6)	88.5	109.1	0.05	-3.27	0.146
Kerlingalaug (7)	48.8	64.5	0.08	-3.52	-0.21
Kerlingalaug (7*)	49	102.6	-0.718	-3.51	0.1
Hólakot (8)	46.4	55.6	0.12	-3.71	-0.293
Reykjarhóll east (9)	61	53.5	0.07	-3.77	-0.313
Reykjarhóll east (9*)	58	103.6	-0.599	-3.74	0.107
Stóra-Brekka (10)	23.8	20.9	0.21	-2.85	-0.664
Stóra-Brekka (10*)	55	92.1	-0.597	-3.423	0.02

Numbers in brackets represent the numbers in ternary diagrams and in Table 1

5.1.5 Component distribution in Fljótin

The distribution of the major elements of geothermal field in the contour map is interpreted with the Surfer 12.6.963 software by Golden Software. The contour map provides useful information for fluid composition distribution and up-flow zone in geothermal field. However, resource management and environment effect will be viable in component distribution map upon utilization of the geothermal field. The selected elements are, SiO_2, CO_2 and Cl. They are selected according to their application in geothermal field where SiO_2 is the indication of heat source, CO_2 describes the size of the reservoir and the major fracture of the geothermal system and Cl indicate the water maturity in the geothermal field.

Component distribution for Fljótin is presented in Figure 11. The SiO_2 concentrations range between 52-148 mg/l in the Fljótin geothermal area. As shown in Figure 11 the concentration of SiO_2 increases from 52 mg/l in the SE (Stóra-Brekka) to NW at Daelir, Bardslaug, Akrar, and Reykjarhóll á Bökkum with SiO_2 concentration range between 136-147 mg/l. The CO_2 concentrations range between 8-24 mg/L increase with the same trend as the silica concentration from SE to NW with the low concentration 8 mg/L at Stóra-Brekka to higher

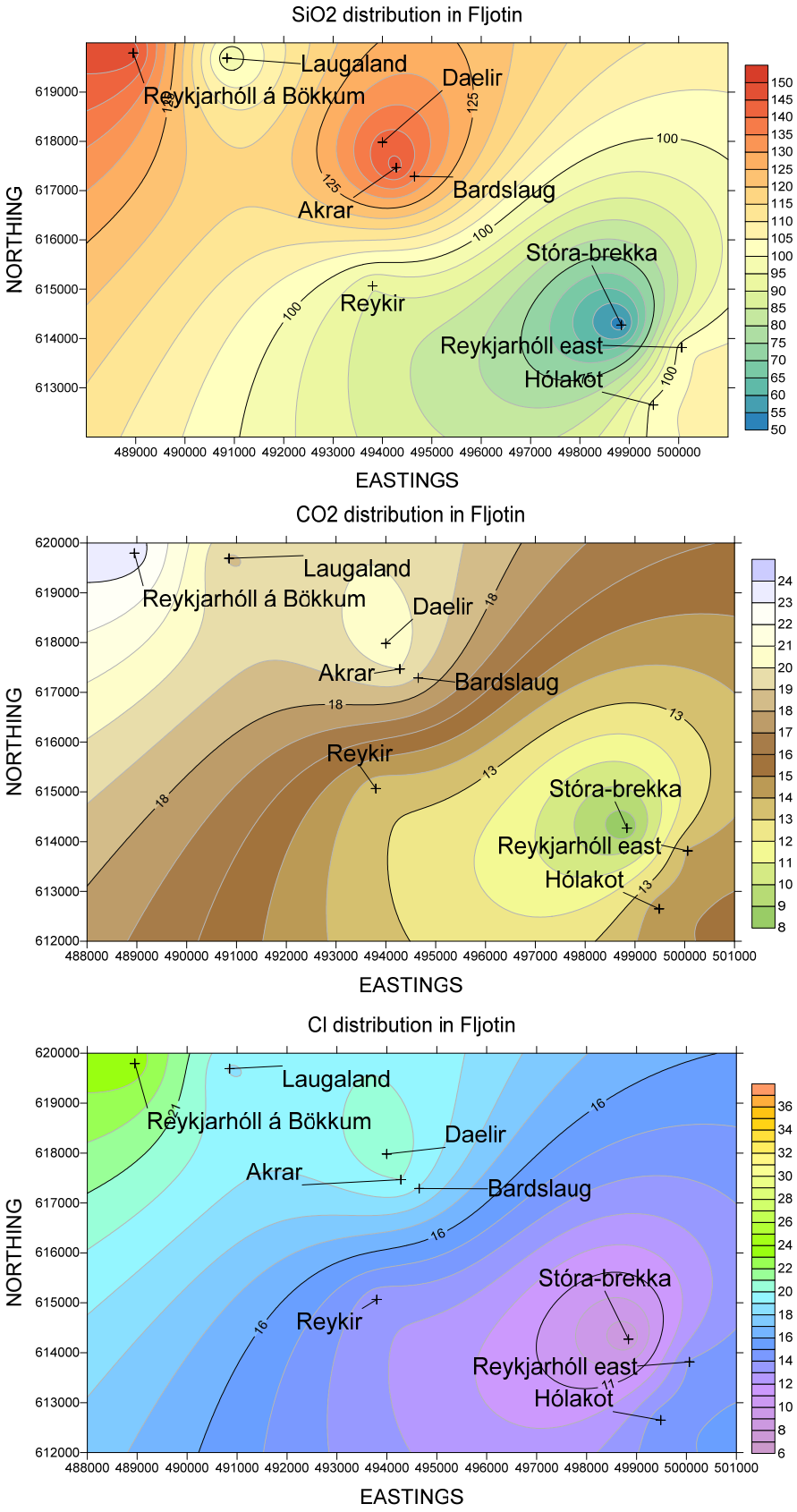

FIGURE 11: Distribution of CO_2, SiO_2, and Cl in Fljótin Iceland

concentration at Reykjarhóll á Bökkum (148 mg/L). The Cl concentration which is very low, range between 9-36 mg/L, increase from 9 mg/L (Reykjarhóll/Hólakot) in the SE towards NW—SE with high concentration of 36 mg/L at Stóra-Brekka and Reykjarhóll á Bökkum.

This SiO_2 concentration is highest between 136-147 mg/l in Daelir, Akrar, Bardslaug and Reykjahóll (the well in the north) which is consistent with the calculated temperature shown in Figure 12.

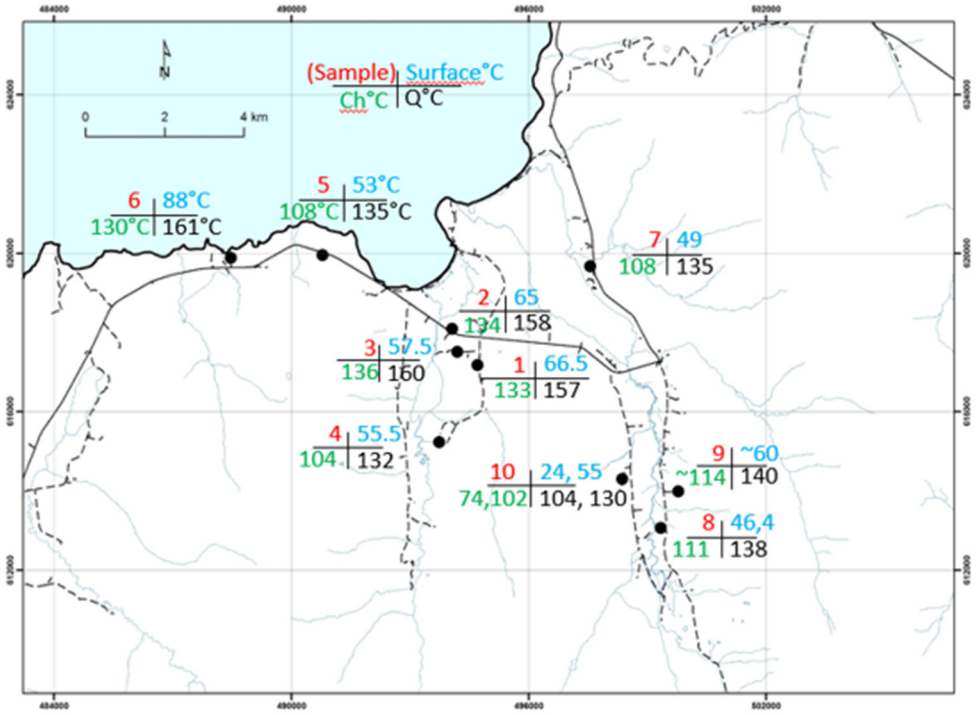

FIGURE 12: Map of Fljótin showing the samples location (number in red) together with measured surface temperature (blue), calculated Chalcedon temperature (green) and calculated quartz temperature

According to geology and chemical analysis of Fljótin, reservoir temperature can be estimated to be 120°C to 160°C. The hot spring is characterized by low temperature geothermal fluid with low enthalpy. Therefore, the area has a potential for direct utilization such as swimming pool, fishing industry, and greenhouses.

5.2 The Rungwe geothermal area

The selected data from Rungwe Tanzania chosen for comparison have been published and interpreted in a report by Ochmann and Garofalo (2013). The selected samples have similar surface temperature as the Fljótin samples. The work on these ten selected samples from the Rungwe volcanic zone (Figure 7) had been done by Bundesanstalt für Geowissenschaften und Rohstoffe (BGR), Sweden Cosultantation Company (SWECO), Icelandic International Development Agency (ICEIDA) and Japan International Cooperation Agency (JICA).

The samples chosen are from the hot springs; Ibayi (a), Ilatile 4 (b), Udindilwa (d), Main Spring (e), Kandete (f), Kasimulo (g), Aqua Afia 3 (h), Aqua Afia1 (i), Swaya (k) and Ikumbi 2 (m). Letters in brackets represent the numbers in ternary diagrams. The samples quality is shown in Table 2, the mineral saturation index is shown in Table 5 and the geothermometers results are shown in Table 6.

The mineral saturation states (index) are expressed by calculated quartz temperature (Fournier and Potter, 1982) where calcite and anhydrite will be saturated while amorphous silica will be supersaturated as is shown Figure 13 and Table 5.

TABLE 5: Mineral saturation state – Rungwe SI index calculated at quartz temperature

Hot spring	Surface temp (°C)	Quartz temp (°C)	Calcite ($CaCO_3$) SI index	Anhydrite ($CaSO_4$) SI index	Amorphous silica (Amr. SiO_2) SI index
Udindilwa (a)	65.7	120.20	-0.980	-2.187	0.017
Ibayi (b)	82.4	126.80	-1.081	-2.152	0.071
Main spring ER (d)	60.3	119.70	-0.758	-2.058	0.012
Aqua Afia 3 (e)	44.1	154.00	-1.100	-4.070	0.28
Aqua Afia 1 (f)	42.4	149.80	-1.250	-4.210	0.249
Ikumbi 2 (g)	44.1	150.20	-1.180	-4.130	0.253
Kandete (h)	56.6	150.50	-0.899	-2.512	0.256
Kasimulo (i)	54.7	139.60	-0.363	-1.840	0.176
Ilatile 4 (k)	80.2	118.60	0.013	-2.256	-0.004
Swaya (m)	44.0	131.20	-0.800	-3.080	0.107

Letters in brackets represent the numbers in ternary diagram and in Table 2

TABLE 6*:* Solute geothertmometers for Rungwe

Sample name	Chalcedony (25-250°C) (1)	Quartz (0-900°C) (2)	K/Mg (°C) (3)
Udindilwa (a)	91.70	120.3	106
Ibayi (b)	98.80	126.8	124
Main Spring (d)	91.00	119.7	121
Aqua Afia 3 (e)	129.00	154.0	120
Aqua Afia1 (f)	124.00	150.0	115
Ikumbi 2 (g)	125.00	150.0	118
Kandete (h)	125.00	150.6	257
Kasimulo (i)	139.90	113.3	252
Ilatile 4 (k)	88.90	117.8	248
Swaya (m)	103.70	131.2	134

Letters in brackets represent the numbers in ternary diagram

1. Arnórsson et al., 1983; 2. Fournier and Potter, 1982; 3. Giggenbach, 1988

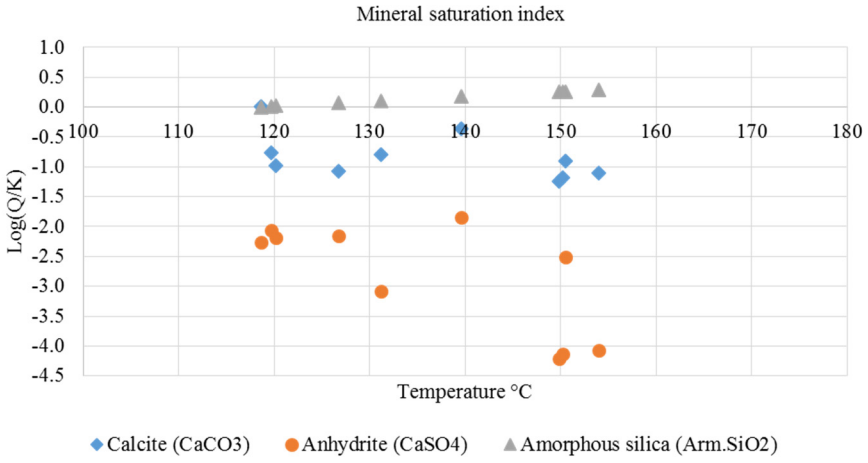

FIGURE 13: Mineral saturation state in Rungwe

The geothermometers used to calculate the reservoir temperature for the Rungwe volcanic zone are quartz, chalcedony, and K/Mg. However, Arnórsson 2000 states that for non-reactive minerals or volcanic system, normally quartz equilibration is used at a temperature less than 100°C. Giggenbach 1986 states that for water with high concentration of Mg, K-M geothermometry will apply for reservoir

estimation temperature. The subsurface temperatures indicate low-temperature geothermal field with confirmation of Na-K-Mg ternary diagram with temperature range of 160-200°C according to geothermometers of quartz and K/Mg with temperature range of 116-154°C and 106-252°C respectively.

5.2.1 Components distribution in Rungwe

The samples were selected in two areas of the geothermal field as indicated in the map: Northern geothermal system (Ngozi-Songwe) and Southern geothermal system (Kiejo-Mbaka) (Ochmann and Garofalo 2013). According to Figure 14 the highest SiO_2 concentration, 105-133mg/l, is in the SE

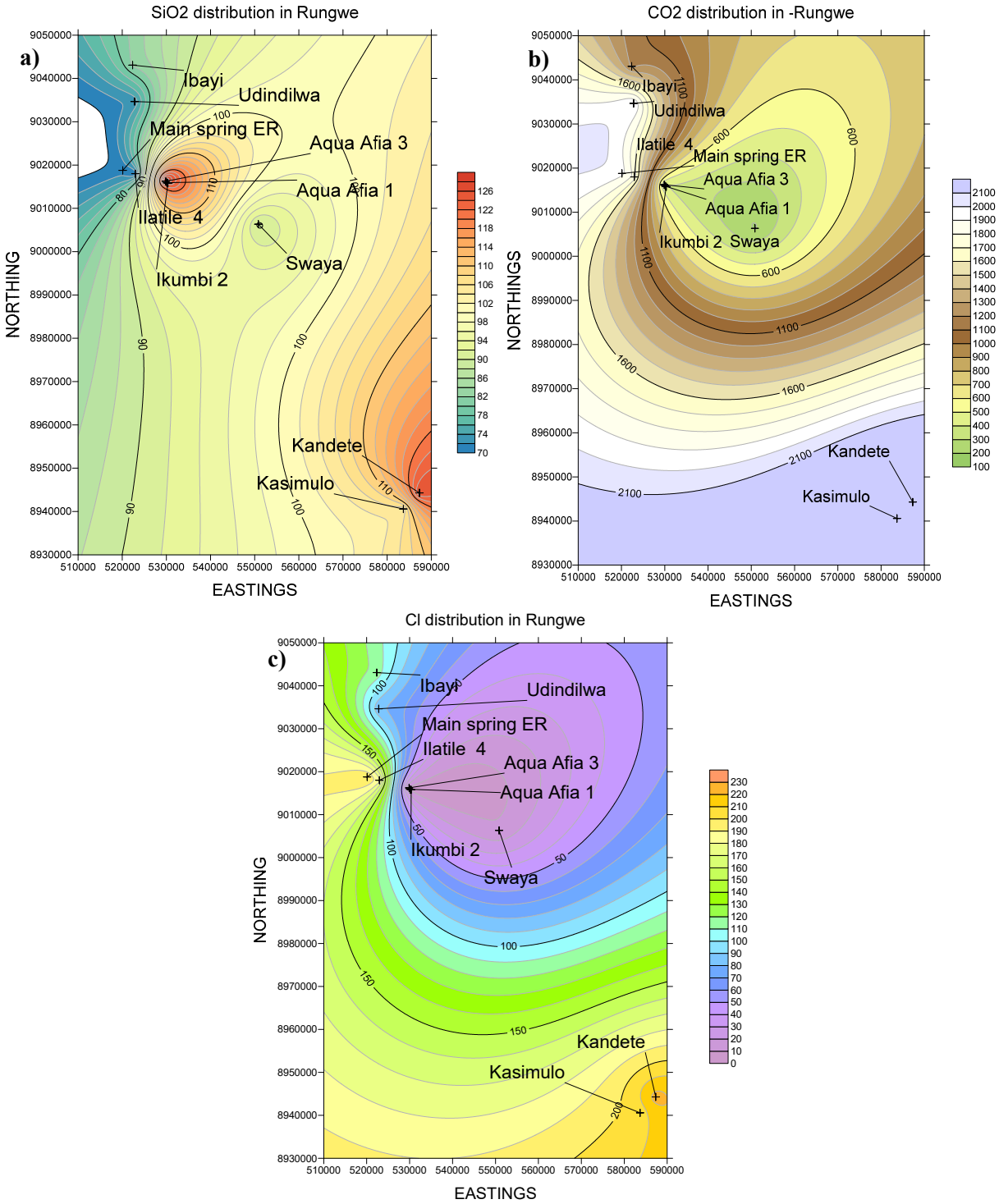

FIGURE 14: Distribution of SiO_2 (a), CO_2 (b), and Cl (c), Rungwe Tanzania

(Kandete and Kasimulo) and in the centre where most of the hot springs are Aqua Afia1, Aqua Afia 3 and Ikumbi 2 locations. In the northern part of the area (Ibayi and Udindilwa), the SiO_2 is lower of ~70-80 mg/l. The trend of CO_2 concentration is increasing towards SE with high concentration of 294mg/l and 295mg/l at Kandete and Kasimulo. The Cl concentration increases on NW-SE direction with high concentration at Main Spring ER, Ilatile 4, Kandete and Kasimulo. From BGR report, Ibayi and Udindilwa have been reported to equilibrate at temperature <200°C (Ochmann and Garofalo 2013).

5.3 Comparison of the Fljótin and the Rungwe geothermal fluids

As written earlier these two geothermal areas are very different both in age and rock composition and therefore the fluid compositions are also very different. The Fljótin a low-temperature geothermal area have estimated reservoir temperature in the range 120°C to 160°C whereas the Rungwe geothermal area reservoir temperature range are in 130°C to 200°C. Rungwe has been divided into two geothermal fields: Northern geothermal system (Ngozi-Songwe) which is high temperature field (>200°C) and Southern geothermal system (Kiejo-Mbaka) which is low-temperature field (<200°C) (Ochmann and Garofalo 2013).

The Fljótin and Rungwe are similar in mineral saturation where both are saturated by amorphous Silica and under saturation calcite and anhydrite are at the estimated reservoir temperature estimated. Fljótin water is classified as low-temperature volcanic water and Rungwe classified as peripheral water with high concentration of HCO_3 as seen in Figure 15. The reservoir temperature for Fljótin can be estimated by chalcedony geothermometer and cation geothermometer in relation with Na-K-Mg ternary diagram. Due to different volcanic activities, rock type and mineral composition (Arnórsson 2000) the chalcedony and Na/K geothermometer has promising result for Fljótin (Table 3), while Rungwe quartz and K/Mg is providing necessary information that compares to other geothermometry (Table 6).

The Fljótin geothermal area and the Rungwe geothermal area are compared on CL-SO_4-HCO_3 ternary diagram shown in Figure 15. According to Ochmann and Garofalo (2013) the selected sample point in Rungwe volcanic zone is classified as low-temperature field (<200) regarding to southern geothermal system with peripheral water characterized by major anion of HCO_3 (blue square) as in Figure 15. The concentration of HCO_3 normally indicate mixing with ground water or mixing of the discharge of CO_2

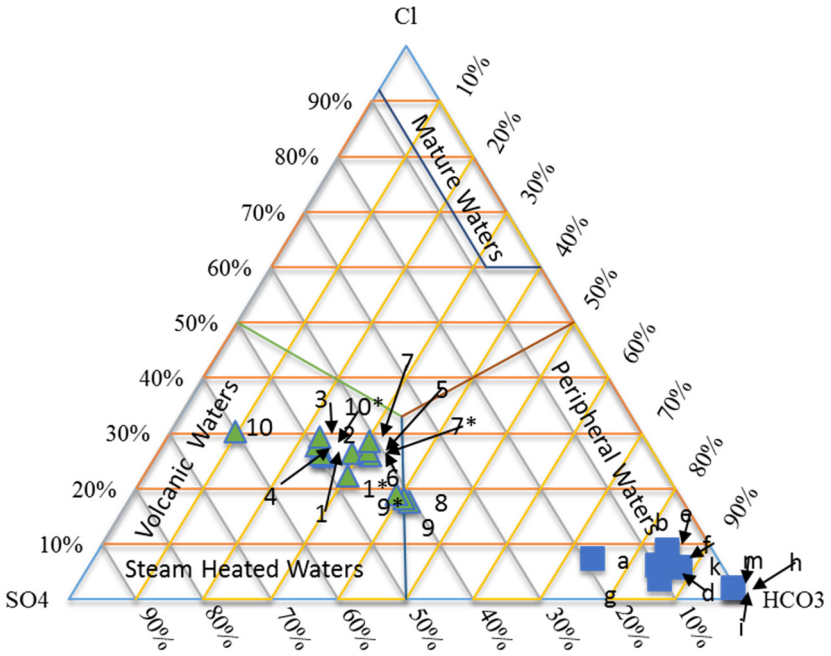

FIGURE 15: Relationship (Comparison) of Fljótin (green triangle) and Rungwe geothermal field samples (blue square) by Cl_SO_4-HCO_3 ternary diagram

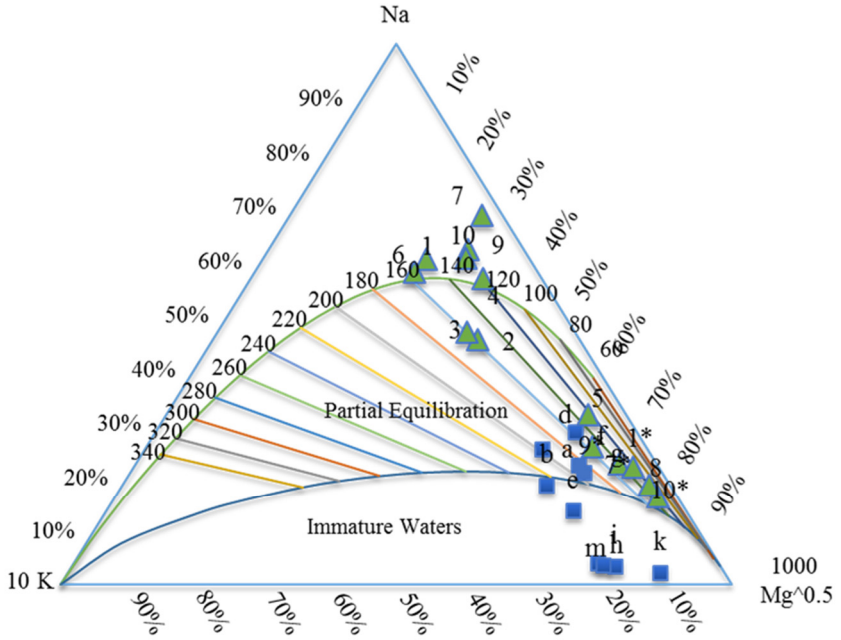

FIGURE 16: Comparisons of the Fljótin samples (green triangle) and the Rungwe samples (blue square) on the Na-K-Mg ternary diagram

from the reservoir interact with ground water fluid at lower temperature (Arnorsson 2000). The Fljótin temperature was estimated at a range of 120°C to 160°C by Na-K-Mg ternary diagram, while in Rungwe volcanic zone the temperature was estimated to be 130°C to 200°C according to the Figure 16 which are confirmed with geothermometers. Geothermometers may provide conclusive information if applied to what is collected as mature water that has reacted with bed rock minerals and reached equilibrium with them.

6. CONCLUSIONS

According to charge balance errors (CBE), sampling collection should be taken by a very keen and skilled person for the purpose of reducing contamination by sampling. The sample quality can contribute to wrong results of geothermal field such as type of fluid, reservoir temperature, size of the reservoir, original of the fluid, the up-flow zone and flow direction.

The Fljótin is a low-temperature geothermal fluid field with low total dissolved elements, low Ca, SiO_2 and CO_2 concentrations, all indicating that the fluid can be used directly without precipitation of calcite and amorphous silica. Fljótin are estimated to have the reservoir temperature range between 120°C-160°C according to chalcedony geothermometer and with temperature range of 64°C-159°C temperature range according to Na/K geothermometer. Which is in agreement with the full equilibrated fluid on the Na-K-Mg ternary diagram. The Fljótin area can be used directly for direct heating, greenhouse industry, aquaculture, fishing industry, tourist attraction like swimming pool and natural bathing.

The Rungwe volcanic zone has been divided into two geothermal fields; Northern geothermal system (Ngozi-Songwe) which is high temperature field (>200°C) and Southern geothermal system (Kiejo-Mbaka) which is low-temperature field (<200°C) (Ochmann and Garofalo 2013). The selected point of thermal water from Rungwe volcanic zone are characterized by Mg-HCO_3 peripheral waters that are partially equilibrated, with estimated reservoir temperature range around 106°C-200°C Although, Rungwe volcanic zone has promising results for a geothermal industry, although Ochmann and Garofalo (2013) report indicate high concentration of CO_2 which will require detailed study in order to reduce the

high operation risk. However, at the moment the field can be used for direct use such as greenhouse, fishing and tourist attraction.

ACKNOWLEDGEMENTS

It gives me great pleasure to extend my sincere gratitude to the UNU-GTP in Iceland and the Ministry of Energy and Minerals, Tanzania. To the UNU-GTP Director Ludvik S. Georgsson, Deputy Director Ingimar G. Haraldsson: thank you for awarding me the opportunity to study in Iceland; Thòrhildur Ísberg, Málfríður Ómarsdóttir and Markús A. G. Wilde: many thanks for facilitating my academic endeavours in Iceland. To all, your ever present support towards the completion of the programme is highly appreciated. To Ministry of Energy and Minerals, my sincere gratitude goes to Permanent Secretary and Commissioner of Energy (CEP) for nominating and granting me permission to attend this vital course. My appreciation to UNU 2015 fellows for laughs and ideas shared during the entire period.

My heartfelt and sincere thanks also go to my supervisor, Dr Vigdís Harðardóttir, for her excellent supervision, fruitful ideas valuable advice and encouragement during the entire project period. Also, my warm thanks go to Gestur Gíslason geochemist at Reykjavík Geothermal, for his constant guidance and knowledge sharing. Appreciation goes to Dr Kristjan Sæmundsson and Dr Halldór Arnórsson for providing useful information for my Project.

Finally, I thank God for keeping health, my lovely kids Clement, Innocent and Eva for the entire period of my study.

REFERENCES

Arnórsson, S., 2000: Mixing processes in upflow zones and mixing models. In: Arnórsson, S. (ed.), *Isotopic and chemical techniques in geothermal exploration, development and use. Sampling methods, data handling, and interpretation*. International Atomic Energy Agency, Vienna, 200-211.

Arnórsson, S., and Andrésdóttir, A., 1995: Processes controlling the distribution of boron and chlorine in natural waters in Iceland. *Geochim. Cosmochim. Acta, 59*, 4125-4146.

Arnórsson, S., Gunnlaugsson, E., and Svavarsson, H., 1983: The chemistry of geothermal waters in Iceland III. Chemical geothermometry in geothermal investigations. *Geochim. Cosmochim. Acta, 47*, 567-577.

Arnórsson, S., Sigurdsson, S. and Svavarsson, H., 1982: The chemistry of geothermal waters in Iceland I. Calculation of aqueous speciation from 0°C to 370°C. *Geochim. Cosmochim. Acta, 46,* 1513-1532.

Arnórsson, S., 1975: Application of the silica geothermometer in low-temperature hydrothermal areas in Iceland. *Am. J. Sci., 275,* 763-783.

Ebinger, C.J., Deino, A.L., Drake, R.E., and Tesha, A.L., 1989: Chronology of volcanism and rift basin propagation: Rungwe volcanic province, East Africa. J. Geophys. Res., 94 B11:15, 785-803.

Ellis, A.J., and Mahon, W.A.J., 1977: *Chemistry and geothermal systems*. Academic Press, New York, 392 pp.

Fournier, R.O., 1977: Chemical geothermometers and mixing model for geothermal systems. *Geothermics, 5,* 41-50.

Fournier, R.O., and Potter, R.W., 1982: An equation correlating the solubility of quartz in water from 25° to 900°C at pressures up to 10,000 bars. *Geochim. Cosmochim Acta, 46*, 1969-1973.

Giggenbach, W.F., 1986: Graphical techniques for the evaluated water/rock equilibration conditions by use of Na, K, Mg and Ca contents of discharge water. *Proceedings of the 8th New Zealand Geothermal Workshop,* 37-43.

Giggenbach, W.F., 1988: Geothermal solute equilibria. Derivation of Na-K-Mg-Ca geoindicators. *Geochim. Cosmochim. Acta, 52*, 2749-2765.

Giggenbach, W.F., 1991: Chemical techniques in geothermal exploration. In: D'Amore, F. (coordinator), *Application of geochemistry in geothermal reservoir development*. UNITAR/UNDP publication, Rome, 119-144.

Gudnason, E.Á., Arnaldsson, A., Axelsson, G., Magnússon, I.Th., Berthet, J.C.C, and Halldórsdóttir, S., 2015: Analysis and modelling of gravity changes in the Reykjanes geothermal field in Iceland, during 2004–2010. *Proceedings of the World Geothermal Congress 2015, Melbourne, Australia*.

Gunnarsson, I. and Arnórsson S., 2000: Amorphous silica solubility and the thermodynamic properties of H_4SiO_4° in the range of 0° to 350°C at P_{sat}. *Geochim. Cosmochim. Acta, 64*, 2295-2307.

Hjartarson, Á. and Sæmundsson, K. 2014: *Geological map of Iceland. Bedrock 1:600 000*. ISOR-Iceland GeoSurvey, Reykjavik.

Jóhannesson, H., 1991: The mountains west of Eyjafjordur, In: *The Icelandic Tourist Association yearbook 1991* (in Icelandic). The Icelandic Tourist Association, Reykjavík, 246 pp.

Kharaka, Y.K., and Mariner, R.H., 1989: Chemical geothermometers and their application to formation waters from sedimentary basins. In: Naesar, N.D. and McCollon, T.H. (editors), *Thermal history of sedimentary basins.* Springer-Verlag, New York, 99-117.

Mwihava, N., 2004: United Republic of Tanzania - Brief on Status of Geothermal Energy. *International Conference "Gethermal Energy Territory" Pemarance, Italy 29-30, Conference Volume* 217-220.

Nicholson, K., 1993: *Geothermal fluids: chemistry and exploration techniques*. Springer-Verlag, Berlin, 268 pp.

Ochmann, N., and Garofalo K., 2013: *Geothermal energy as alternative source of energy for Tanzania.* BGR Final Report.

Pope, L.A., Hajash, A., and Popp, R.K., 1987: An experimental investigation of the quartz, Na-K, Na-K-Ca geothermometers and the effect of fluid composition. *J. Volcanol. Geotherm. Res., 31*, 151-161.

Saemundsson, K., 1979: Outline of the geology of Iceland. *Jökull 29,* 7-28.

Schlitzer, R., Roether, W., Weidmann, U., Kalt, P., and Loosli, H. H., 1985: A meridional 14C and 39Ar section in northeast Atlantic deep water. *Journal of Geophysical Research: Oceans (1978–2012)*, *90*(C4), 6945–6952.

Sekento, L. R.., 2012: Geochemical and isotopic study of the Menengai geothermal field, Kenya. Report 31 in: *Geothermal Training in Iceland 2012*. UNU-GTP, Iceland, 769-792.

Verma, S.P., and Santayo, E., 1997: New improved equations for Na/K, Na/Li and SiO_2 geothermometers by outlier detection and rejection. *J. Volcanol. Geotherm. Res., 79*, 9-23.

Verma, M.P., 2000: Chemical thermodynamics of silica: a critique on its geothermometer, *Geothermics 29*, 323-346.